Effective dimensions and chemical reactions in fluid flows

György Károlyi*
Centre for Applied Dynamics Research, School of Engineering and Physical Sciences, University of Aberdeen, King's College, Aberdeen AB24 3UE, Scotland, United Kingdom

Tamás Tél
Institute for Theoretical Physics, Eötvös University, P.O. Box 32, H-1518 Budapest, Hungary
(Received 22 June 2007; published 25 October 2007)

We show that chemical activity in hydrodynamical flows can be understood as the outcome of three basic effects: the stirring protocol of the flow, the local properties of the reaction, and the global folding dynamics which also depends on the geometry of the container. The essence of each of these components can be described by simple functional relations. In an ordinary differential equation approach, they determine a new chemical rate equation for the concentration, which turns out to be coupled to the dynamics of an effective fractal dimension. The theory predicts an exponential convergence to the asymptotic chemical state. This holds even in flows characterized by a linear stirring protocol where transient fractal patterns are shown to exist despite the lack of any chaotic set of the advection dynamics. In the exponential case the theory applies to flows of chaotic time dependence (chaotic flows) as well.

DOI: 10.1103/PhysRevE.76.046315 PACS number(s): 47.52.+j, 47.54.Fj, 05.45.−a, 47.53.+n

I. INTRODUCTION

There is increasing interest in the experimental investigation of chemical reactions in flows whose advection dynamics is chaotic. After an early attempt [1], recent studies investigate reactions in the blinking vortex flow [2], in a cellular flow [3], and in an electrolytic flow [4]. The type of reactions ranges from excitable media, via autocatalytic and acid-base reactions to oscillating reactions [5]. This development has been preceded by a series of theoretical works [6–22] (for a review see Ref. [23]).

The reaction kinetics depends essentially on whether the flow is closed or open: in the case of open flows there is a current flowing through the region of observation, while in the case of closed flows there is no escape from a bounded region. One observes a basic dichotomy between the reaction-free advection dynamics in open and closed flows, as shown in Table I. In open flows there is a time-independent fractal dimension associated with the chaotic advection dynamics. The chaotic advection dynamics itself is, however, unavoidably transient, i.e., of finite lifetime. In closed flows chaos is permanent, but produces structures whose degree of filamentarity changes in time. Hence fractality is of transient character in this second case.

Experiments usually take place in closed containers. In the absence of fluid transport barriers simple reactions lead to a steady state in which the full fluid domain is either occupied by the product or no product is present at all. The asymptotic state is thus homogeneous, and hence much less interesting than in the open case. Before reaching the asymptotic state, the chemical product appears, however, to have filamentary features (see Figs. 2 and 5), and the process can be understood by methods applied earlier to open flows [23].

We propose to characterize chemical transients in closed containers by means of a time-dependent effective dimension $D_{\mathrm{eff}}(t)$. This concept has been used in other contexts [24–28] and also in relation to chemical reactions in flows [9,15]. Our paper extends the results of [15] from periodic flows to those with chaotic time dependence (random flows), to several types of reactions and to different stirring protocols.

Special emphasis is devoted to flows not generating chaotic advection. As pointed out in Refs. [29–31], a linear protocol (linear growth of line segments) can characterize remarkable complex passive scalar patterns. One therefore expects the reactions to spread along filamentary patterns in this case as well. The experiments of Rogers and Morris [32] with vortex rings and reactions provide evidence for this view. Recent numerical simulations [33,34] show reaction enhancement even in the flow of a single vortex. The concept of an effective dimension is therefore applicable to such cases too.

We derive a coupled set of equations between the time evolution of the chemical products and of the effective dimension. We point out that the convergence towards the homogeneous steady state is exponential with an exponent that might be different from the Lyapunov exponent of the advection dynamics in chaotic flows. An interesting feature of the nonchaotic case is that the long time asymptotics is exponential in spite of the absence of any chaos in the underlying advection dynamics. The lack of chaos is reflected in the fact

TABLE I. Basic difference between properties of open and closed flows.

	Open flow	Closed flow
chaos	transient	permanent
fractality	permanent	transient

*Permanent address: Center for Applied Mathematics and Computational Physics, and Department of Structural Mechanics, Budapest University of Technology and Economics, Műegyetem rkp. 3., H-1111 Budapest, Hungary.

that the value of the effective dimension in the asymptotic state is an integer, smaller than the dimension of the fluid domain. For reactions with initially one-dimensional interface in a closed container, the growth is typically linear in time, independently of the stirring protocol.

Much insight can be gained into any kind of reaction dynamics by analyzing the so-called Lagrangian filament slice model [8]. The idea is to investigate a long, straight segment of a filament along which stretching takes place. The reaction is followed perpendicular to this segment only since, due to stretching, the distribution can be considered to be homogeneous along the filament. This property is best fulfilled for the exponential protocol, nevertheless, we assume that it holds for any type of sufficiently strong stretching. The effect of the flow transverse to the filament is a local contraction. In chaotic flows these filaments are subsets of the unstable manifold of a chaotic set, and contraction is then governed by the contracting Lyapunov exponent. We shall use the simplest version of this model when the dynamics can be described by ordinary differential equations [35].

The paper is organized as follows. In Sec. II the basic mechanisms: the stirring protocols, the reactions, and the global folding dynamics are formulated. The time evolution of the concentration and the dimension are derived in Sec. III. Next, in Sec. IV, we present numerical evidence in support of the theory. The open flow case is revisited in Sec. V and our conclusions are drawn in Sec. VI.

II. FILAMENTS IN CLOSED FLOW

For simplicity, we consider two-dimensional flows, as in experiments [1–5]. Our approach is based on three different levels of description: the stirring protocol (a feature of the passive advection in the reaction-free flow) expressed as a stretching and contraction process, the chemical reaction which modifies the contraction dynamics locally (in the spirit of the Lagrangian filament slice model), and the global folding process which leads to saturation (a feature in which the shape of the container also plays a role). These different levels are characterized by the protocol, reaction and folding functions, p (protocol), r (reaction), and f (folding), respectively, to be defined below.

Based on the local properties expressed by p and r, and the global property of folding, a time-dependent effective dimension D_{eff} can be defined whose dynamics is coupled to that of the chemical concentration c. Both dynamics will be shown to be essentially determined by the functions p, r, and f. Up to Sec. V only closed flows will be considered.

A. Local properties

In the lack of activity, the flow cannot change the material content in a closed container. Stretching and folding actions of the flow distort an initial patch of material into filaments of width $\delta(t)$ and total length $\mathcal{L}(t)$. Due to incompressibility, the total covered area remains constant, $\mathcal{L}\delta=\mathrm{const}$, hence $\dot{\mathcal{L}}\delta+\mathcal{L}\dot{\delta}=0$. We can rewrite this in dimensionless form using $d=\delta/L$, $l=\mathcal{L}/L$ with L as a characteristic linear size of the system and get $\dot{d}l+d\dot{l}=0$.

The stirring process defines an instantaneous stretching rate via $\dot{l}(t)/l(t)$. This can be written as an overall constant rate λ (of dimension 1/time) times a function $p(t)$. In our mean-field-type theory, the fluctuations of this rate are neglected. The protocol function $p(l)$ is obtained by eliminating t in terms of the instantaneous length l. Thus

$$\frac{\dot{l}}{l}=\lambda p(l). \tag{1}$$

Note that the instantaneous contraction rate $\dot{d}/d$ of the reaction free flow is $-\lambda p(l)$, due to area preservation.

Stirring protocols of particular interest are the exponential stretching and the linear stretching. The exponential protocol is typical for chaotic advection with λ as the average Lyapunov exponent. In the linear protocol [29–31] $\dot{\mathcal{L}}=\lambda'$, with λ' as a constant growth velocity. Therefore, $\dot{l}=\lambda'/L \equiv \lambda$. The particular protocol functions are thus

$$p(l)\equiv 1 \quad \text{and} \quad p(l)=\frac{1}{l} \tag{2}$$

for exponential and for linear stirring, respectively.

The basic effect of reaction is a modification of the contraction dynamics. We consider two different types of reactions.

The first example is reactions with front propagation, e.g., autocatalytic reactions $A+C\rightarrow 2C$. In such cases material C is spreading into the medium of material A with a constant front velocity v and behind the front the concentration of C is approximately a constant $\bar{c}$. The width δ of the band [see Fig. 1(a)] in which material C is distributed along the stretching direction increases therefore with the speed of $2v$. The dynamics of the dimensionless width $d=\delta/L$ is thus

$$\dot{d}=-\lambda p(l)d+2v/L. \tag{3}$$

This equation is expected to be valid for any reaction with frontal propagation. According to Luther's law [36], the front velocity is proportional to the square root of the reaction rate k and of the diffusion coefficient D_{diff}:

$$v=\alpha(kD_{\mathrm{diff}})^{1/2}. \tag{4}$$

With α of order unity, this law holds for an amazing variety of reactions ranging from bistable and excitable ones to flames [36] and models of epidemics [37].

In the case of an acid-base type reaction $A+B\rightarrow 2C$, we imagine that components A and B are distributed uniformly on the two sides of the filament and reaction takes place within bands of average width $\delta(t)$ as sketched in Fig. 1(b). Inside this band the C concentration is assumed to be a constant $\bar{c}$. The width is changing due to diffusion with a rate D_{diff}/δ. Note that $\dot{\delta}=D_{\mathrm{diff}}/\delta$ has the usual $\delta=(\delta_0^2+2D_{\mathrm{diff}}t)^{1/2}$ solution, but this is counteracted by the simultaneous presence of contraction due to the flow. The full dynamics of the bandwidth $d=\delta/L$ is therefore governed by

$$\dot{d}=-\lambda p(l)d+D_{\mathrm{diff}}/(L^2 d). \tag{5}$$

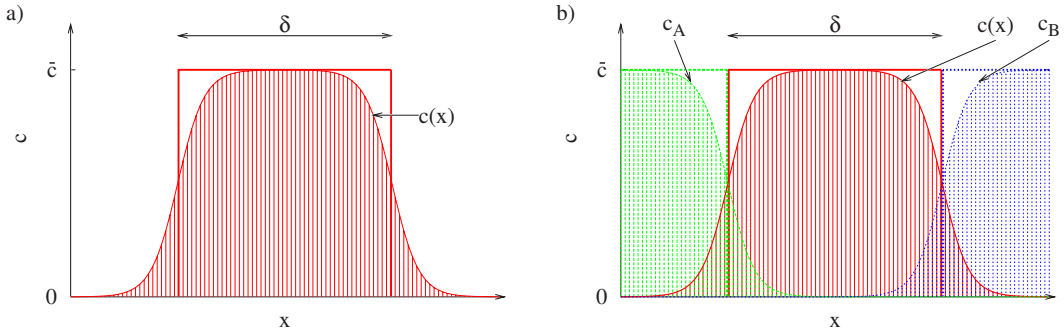

FIG. 1. (Color online) Concentration distribution $c(x)$ of material C (dashed central peaks, red online) along the contracting direction x of the flow and the definition of the bandwidth $\delta(t)$. (a) Autocatalytic reaction, material A is in abundance outside of C. The transition region, the reaction front, is propagating with a fixed velocity v relative to the fluid. (b) Acid-base reaction. The motion of the transition region, relative to the flow, is due to diffusion; there is no intrinsic front velocity v in this case. If the transition region between material C and the other components is narrow enough, the concentration of material C can be well approximated by a function which is constant (of value $\bar{c}$) over an interval of length $\delta(t)$, and zero outside. Concentrations are considered here as number densities.

We can unify and generalize the reaction schemes described by Eqs. (3) and (5) by writing

$$\dot{d} = -\lambda p(l) dr(d,l), \tag{6}$$

where the reaction function $r(d,l)$ is dimensionless. The presence of r expresses the renormalization of the contraction dynamics due to the reaction. The particular forms from Eqs. (3) and (5) are

$$r(d,l) = 1 - \frac{2U}{p(l)d} \quad \text{and} \quad r(d,l) = 1 - \frac{1}{\mathrm{Pe}p(l)d^2} \tag{7}$$

for autocatalytic and acid-base reactions, respectively. Here $\mathrm{Pe}=L^2\lambda/D_{\mathrm{diff}}$ is the (Lagrangian) Péclet number, $U=v/(\lambda L)$ is a dimensionless front velocity, which can be written in view of Eq. (4) as $U=\alpha(\mathrm{Da}/\mathrm{Pe})^{1/2}$ with $\mathrm{Da}=k/\lambda$ as the (Lagrangian) Dahmköhler number [23]. Equation (7) shows that acid-base type reactions are basically diffusion limited: no Dahmköhler number appears in the reaction function.

We assume that a steady state solution $d^*>0$ exists for which

$$r(d^*,l^*) \equiv 0, \tag{8}$$

and the steady state is stable. The steady state bandwidth for the exponential stirring protocol is

$$d^* = 2U \quad \text{and} \quad d^* = \mathrm{Pe}^{-1/2} \tag{9}$$

for frontal and for acid-base reactions, respectively. For the linear stirring protocol we get

$$d^* = 2Ul^* \quad \text{and} \quad d^* = (l^*/\mathrm{Pe})^{1/2} \tag{10}$$

in the case of frontal and acid-base reactions, respectively. In these forms l^* is the length of the filaments when saturation sets in.

In a container of area $\mathcal{H}L^2$ (for a circular dish of radius $L=R$ the prefactor is, for instance, $\mathcal{H}=\pi$), the total length at saturation is $\mathcal{L}^*=\mathcal{H}L^2/\delta^*=\mathcal{H}L/d^*$. This implies $l^*=\mathcal{H}/d^*$, which fixes the steady state bandwidths for the linear protocol in view of Eq. (10) as

$$d^* = (2U\mathcal{H})^{1/2} \quad \text{and} \quad d^* = (\mathcal{H}/\mathrm{Pe})^{1/3} \tag{11}$$

for autocatalytic and acid-base reactions, respectively. Pronounced filamentarity is present if the dimensionless bandwidth is small, that is if

$$U \ll 1 \quad \text{and} \quad \mathrm{Pe} \gg 1, \tag{12}$$

which we assume in what follows.

B. Global properties

As a simple though general form, we write the equation for the dimensionless length $l=\mathcal{L}/L$ as

$$\dot{l} = \lambda p(l) l f\left(\frac{\mathcal{L}}{\mathcal{L}^*}\right) = \lambda p(l) l f\left(\frac{ld^*}{\mathcal{H}}\right). \tag{13}$$

In contrast to p and r, we do not specify the form of the folding function $f(\mathcal{L}/\mathcal{L}^*)>0$, but require $f(0)=1$ and $f(1)=0$ to ensure an initial growth with an asymptotic saturation. Equation (13) can be interpreted as the renormalized form of the stretching dynamics (1) due to the finite size of the container.

Fractal dimension of curves can be considered as a measure of their foldedness. Since a long line can fit into a finite area only if it is strongly folded, we define an instantaneous effective dimension $D_{\mathrm{eff}}(t)$ by counting the number N of boxes needed to cover all the bands containing product C with boxes of size $d(t)$, and requiring that it scales as a power of d: $N(d)=\mathcal{H}d^{-D_{\mathrm{eff}}}$ $(1\leqslant D_{\mathrm{eff}}\leqslant 2)$. Note that d here is not arbitrarily small, it is given by Eq. (6). The total length $l \approx Nd$ can then be written as

$$l(t) = \mathcal{H}d(t)^{1-D_{\mathrm{eff}}(t)}. \tag{14}$$

The product content in the container is $C(t)=\bar{c}\mathcal{L}\delta=\bar{c}L^2ld=\bar{c}L^2\mathcal{H}d(t)^{2-D_{\mathrm{eff}}(t)}$, where $\bar{c}$ is the concentration inside the bands. The average dimensionless concentration is then $c(t)=C(t)/(\bar{c}\mathcal{H}L^2)$, and we find that

$$c(t) = d(t)l(t)/\mathcal{H} = d(t)^{2-D_{\mathrm{eff}}(t)}. \tag{15}$$

From here

$$d(t) = c(t)^{1+\beta(t)}, \quad l(t) = \mathcal{H}c(t)^{-\beta(t)}, \tag{16}$$

where notation

$$\beta(t) \equiv \frac{D_{\text{eff}}(t) - 1}{2 - D_{\text{eff}}(t)} \tag{17}$$

has been introduced.

III. DIMENSION AND CONCENTRATION IN CLOSED FLOWS

By taking the time derivative of the left equality of Eq. (15) and using Eqs. (6), (13), and (16), we obtain

$$\dot{c} = -c\lambda p(\mathcal{H}c^{-\beta})[r(c^{1+\beta}, \mathcal{H}c^{-\beta}) - f(c^{-\beta}d^*)]. \tag{18}$$

It is remarkable that a negative power $(-\beta)$ of the average concentration occurs in the chemical rate equation (just as in open flows [7,23]).

Differentiating the right equality of Eq. (15), and using Eqs. (6) and (18), an equation for the effective dimension follows:

$$\dot{D}_{\text{eff}} \ln d = (D_{\text{eff}} - 1)\lambda pr - \lambda pf. \tag{19}$$

In terms of exponent β,

$$\dot{\beta} = \frac{\dot{D}_{\text{eff}}}{(2 - D_{\text{eff}})^2} = \frac{\lambda p(\mathcal{H}c^{-\beta})}{\ln c}[\beta r(c^{1+\beta}, \mathcal{H}c^{-\beta}) - (1+\beta)f(c^{-\beta}d^*)]. \tag{20}$$

Equations (18) and (20) yield a coupled set of equations for the concentration c and the dimension-determined exponent β.

During the initial period, we can assume that $f \approx 1$ since saturation is not yet in effect. If the product is distributed along a line initially, so that the effective dimension is $D_{\text{eff},0} = 1$, implying $\beta_0 = 0$, we find from Eq. (18)

$$\dot{c} = \lambda c p(\mathcal{H})[1 - r(c, \mathcal{H})]. \tag{21}$$

For frontal reactions, substituting here from Eq. (7) the form $r = 1 - 2U/[p(\mathcal{H})c]$ we find $\dot{c} = 2U\lambda$, implying a linear growth

$$c(t) = c_0 + 2U\lambda t. \tag{22}$$

For an acid-base reaction [see Eq. (7)], the initial behavior is $r = 1 - 1/[c^2 p(\mathcal{H})\text{Pe}]$, thus $\dot{c} = \lambda/(c\text{Pe})$, leading to a diffusive growth

$$c(t) = (c_0^2 + 2\lambda t/\text{Pe})^{1/2} \approx c_0 + \frac{\lambda t}{c_0 \text{Pe}}. \tag{23}$$

Note that these initial rules are independent of the stirring protocol. An exponential growth would only follow for an initial distribution of negligible bandwidth ($d_0 = 0$) which quickly turns into Eqs. (22) or (23).

In order to see how the trivial $c \to c^* \equiv 1$, $D \to 2$, $d \to d^*$ final state is reached, we take into account Eq. (16), the identity $c^{-\beta}d^* \equiv cd^*/d$, and linearize Eqs. (6) and (18) as

$$\dot{d} = -\lambda p^* \left(y d^* - z \frac{\mathcal{H}}{d^*} \right)(d - d^*) - \lambda p^* z \mathcal{H}(c - 1), \tag{24}$$

$$\dot{c} = -\lambda p^* (y - z\mathcal{H}/d^{*2} - a/d^*)(d - d^*) - \lambda p^* (z\mathcal{H}/d^* + a)(c - 1), \tag{25}$$

where notations $p^* \equiv p(l^*)$, $a \equiv -f'(1)$, $y \equiv \partial r/\partial d(d^*, l^*)$, and $z \equiv \partial r/\partial l(d^*, l^*)$ have been introduced. In addition to the derivatives of known functions, a single phenomenological parameter appears: the derivative a of the saturation function in the steady state.

From Eq. (19)

$$\dot{D}_{\text{eff}} = \frac{\lambda p^*}{\ln d^*}[(y - z\mathcal{H}/d^{*2} - a/d^*)(d - d^*) + (z\mathcal{H}/d^* + a)(c - 1)], \tag{26}$$

which shows that the dynamics of the effective dimension D_{eff} simply follows the dynamics of the average concentration c: as we approach the steady state.

The convergence $c \to 1$ is governed by the largest of the eigenvalues of the Jacobian in Eqs. (24) and (25). The eigenvalues turn out to be $-a\lambda p^*$ and $-yd^*\lambda p^*$. Note that they are independent of parameter z. Hence we have

$$1 - c \sim \exp(-\sigma t), \quad 2 - D_{\text{eff}} \sim \exp(-\sigma t), \tag{27}$$

with the chemical decay rate

$$\sigma = \min\{a\lambda p^*, yd^*\lambda p^*\}. \tag{28}$$

In the particular case of the exponential protocol $p^* \equiv 1$. From Eqs. (7) and (9) we obtain the decay rate as

$$\sigma = \lambda \min\{a, 1\} \tag{29}$$

for the autocatalytic and

$$\sigma = \lambda \min\{a, 2\} \tag{30}$$

for the acid-base reaction. These imply

$$\sigma \leqslant \lambda \quad \text{and} \quad \sigma \leqslant 2\lambda \tag{31}$$

for these two types of reactions. Since only the stirring protocol is important, the theory applies to flows of chaotic time-dependence (random flows) as well.

For the linear protocol $p^* = 1/l^* = d^*/\mathcal{H}$ and, using Eqs. (7) and (11), we obtain

$$\sigma = \lambda \left(\frac{2U}{\mathcal{H}} \right)^{1/2} \min\{a, 1\}, \tag{32}$$

$$\sigma = 2\lambda(\mathcal{H}^2\,\text{Pe})^{-1/3} \min\{a, 2\} \tag{33}$$

for the autocatalytic and the acid-base reactions, respectively.

The decay rate is on the order of the Lyapunov exponent (a is a dimensionless number) for the exponential protocol (i.e., chaotic flows). For the linear protocol, it is determined by the linear stretching rate but also depends on the front velocity (frontal reactions) and on the strength of the diffusion (acid-base reactions).

IV. NUMERICAL RESULTS

The flow we used to model the exponential stirring protocol (chaotic advection) is a random sinusoidal shear flow in alternating directions in a unit square with periodic boundary conditions [38]. The velocity of the flow is

$$v_x(x,y,t) = A\Theta\left(\frac{1}{2} - t \bmod 1\right)\sin(2\pi y + \varphi_i),$$

$$v_y(x,y,t) = A\Theta\left(t \bmod 1 - \frac{1}{2}\right)\sin(2\pi y + \varphi_{i+1}), \quad (34)$$

where Θ is the Heaviside step function, and A is the parameter that controls the chaotic behavior of the flow. Setting φ_i to be a random phase in each half time period, it is possible to avoid the existence of transport barriers (in the form of KAM tori [39] typically present in a periodically driven conservative system). The exponential stirring protocol is achieved by using this random phase and $A=0.7$ as the flow parameter.

The linear stirring protocol was investigated in the velocity field generated by two point vortices of circulation $\Gamma_1 = \Gamma = -\Gamma_2$ moving in the (x,y) plane [40]. Starting at $t=0$ from $(-a,0)$ and $(a,0)$, the vortex pair moves with a velocity $\Gamma/(2a\pi)$ along the y axis: $x_1(t) \equiv -a$, $x_2(t) \equiv a$ and $y_1(t) = y_2(t) = \Gamma t/2a\pi$. The velocity field for a passively advected particle at a point (x,y) can be written as

$$v_x(x,y,t) = \frac{\partial \Psi(x,y,t)}{\partial y}, \quad v_y(x,y,t) = -\frac{\partial \Psi(x,y,t)}{\partial x}, \quad (35)$$

where

$$\Psi(x,y,t) = -\frac{1}{\pi}\sum_{i=1}^{2} \Gamma_i \ln r_i(x,y,t) \quad (36)$$

is the stream function [40]. Here r_i is the distance of point (x,y) from the center $[x_i(t), y_i(t)]$ of vortex i. Using dimensionless units, the vortices initially located at $(-1,0)$ and $(1,0)$ have vortex strength 1 and -1, respectively. In a frame of reference comoving with the vortices the velocity field of the advected particles becomes stationary:

$$v_x(x,y) = \frac{y}{(x-1)^2 + y^2} - \frac{y}{(x+1)^2 + y^2},$$

$$v_y(x,y) = \frac{x+1}{(x+1)^2 + y^2} - \frac{x-1}{(x-1)^2 + y^2} - \frac{1}{2}. \quad (37)$$

To simulate the reactions, the region of observation (the unit square in the case of the random sinusoidal shear flow, and the square $[-3,3]\times[-3,3]$ in the case of the point vortexes) was covered with a grid. Each grid cell could only be occupied by a maximum of one particle. In the random sinusoidal shear flow, reaction events occurred after each half period, when the flow changed direction. In the case of the vortex flow, reaction events occurred at integer multiples of a time lag 0.1. For frontal reactions ($A+C \to 2C$), initially one reacting particle was placed in each grid-cell of a narrow band across the fluid [see Fig. 2(a)], and at the reaction events all occupied grid-cells "infected" all their neighbors. For acid-base reactions ($A+B \to 2C$), initially the two reactants A and B occupied the left and right halves of the unit square [as in Fig. 5(a)]. At the reaction events, if both A and B types of particles were present in a block of 2×2 grid cells, then in each grid cell in this block a product particle (C) was placed.

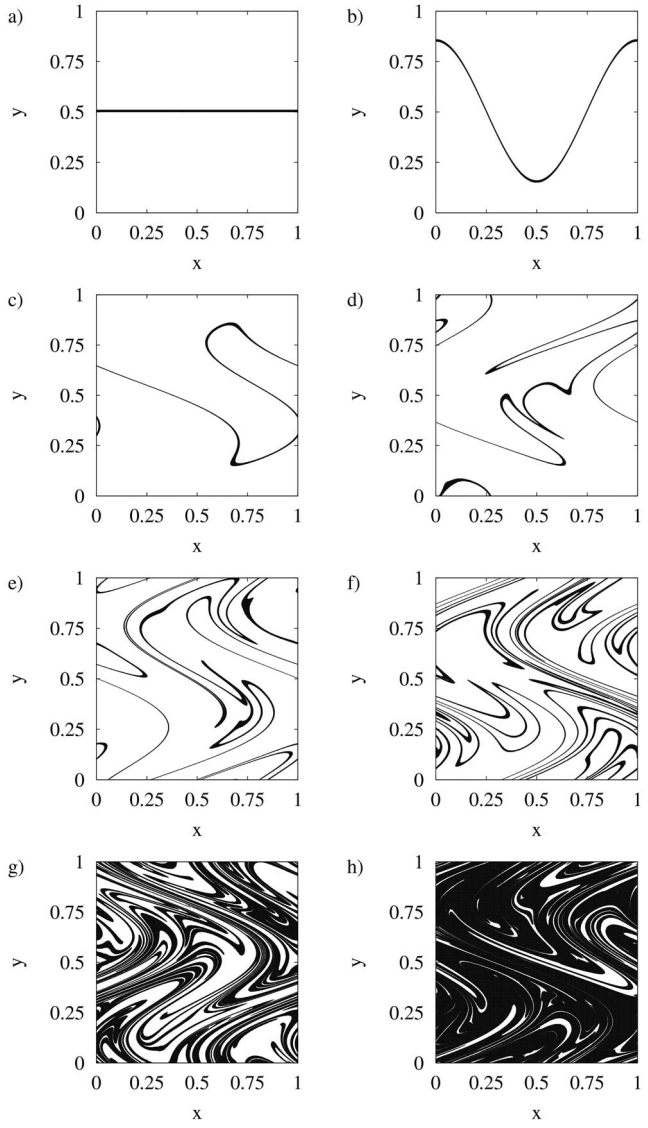

FIG. 2. Distribution of the autocatalytic C particles (black) in the random sinusoidal shear flow, with $A=0.7$ in Eq. (34). The simulations were performed on a grid of size 1024×1024. Reactions occurred at each half period of the flow, when the direction of the flow velocity changed. The snapshots are shown at (a) 0, (b) 0.5, (c) 1, (d) 2, (e) 3, (f) 4, (g) 6, (h) 8 periods, right before the reaction events.

In Fig. 2 we show a series of snapshots of the autocatalytic process in the case of the exponential stirring protocol. The distribution of C particles, initially a straight line, is stretched and folded by the fluid mixing, while the chemical activity does not allow the stripe width to shrink. As a consequence, the whole domain becomes covered by the product eventually, and the reaction stops. Before that, however, the

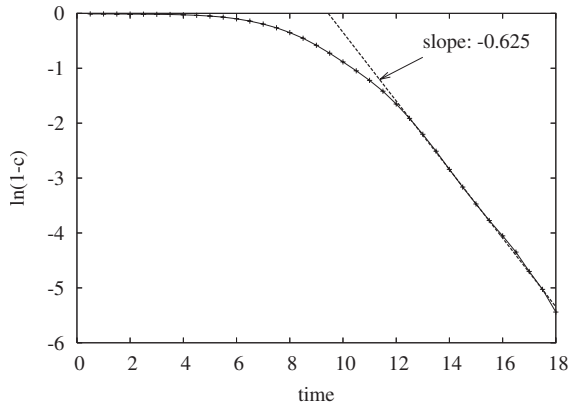

FIG. 3. Concentration c of reactant C in the autocatalytic reaction of Fig. 2. Time is measured in periods of the flow, concentration is sampled just before the reaction events. The simulations were performed on a grid of size 8192×8192. The average Lyapunov exponent of the flow is $\lambda=0.60\pm0.02$. Crosses represent results obtained from the simulation, the straight line is predicted by Eq. (27). The chemical decay rate from the plot is $\sigma=0.625\pm0.006$.

reaction takes place along a filamentary structure.

The average concentration of the autocatalytic particles as a function of time is well predicted by Eq. (27), as illustrated in Fig. 3. From this figure, we find that the chemical decay rate σ in Eq. (27) becomes $\sigma=0.625\pm0.006$, approximately equal to the average Lyapunov exponent $\lambda=0.60\pm0.02$.

In Fig. 4 the prediction (27) for the effective dimension is verified in the large t regime. The effective dimension was measured by the standard box-counting method. In principle, $D_{\text{eff}}(t)$ is defined as the tangent of the ln N(eps) vs ln eps curve at $\varepsilon=d(t)$, where ε is the box size, and $N(\varepsilon)$ is the number of boxes of size ε necessary to cover all the filaments. In our case, however, the range of fractal scaling extends over more than a decade. An example is shown in the inset of Fig. 4. From the figure we found $\sigma=0.639\pm0.007$, which is close to the decay rate obtained from the concentration.

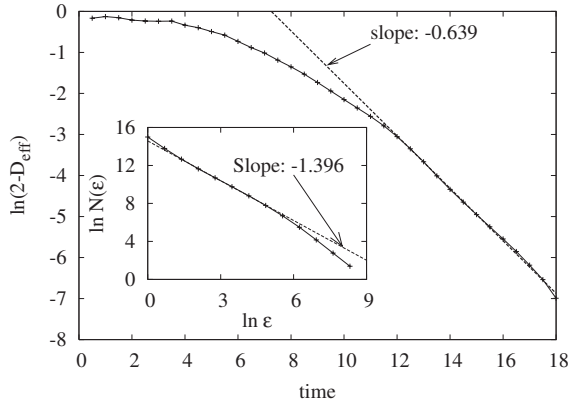

FIG. 4. Time dependence of the effective dimension in the numerical experiment of Fig. 3. Crosses represent the measured D_{eff} values, while the straight line is predicted by Eq. (27). The chemical decay rate is $\sigma=0.639\pm0.007$. An illustration of the box counting algorithm is shown in the inset, where the data correspond to time $t=5$, before the reaction event.

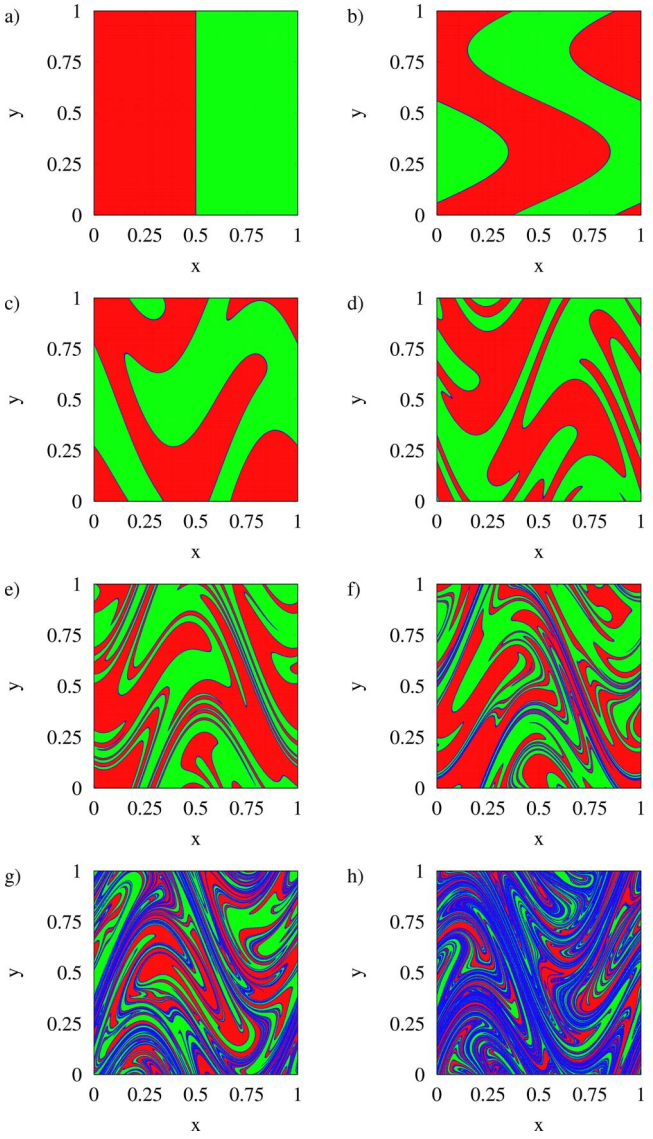

FIG. 5. (Color online) Distribution of materials A (medium gray, red online), B (light gray, green online) and C (dark gray, blue online) of the acid-base reaction $A+B\rightarrow2C$ in the random sinusoidal shear flow with $A=0.7$ in Eq. (34). The simulations were performed on a grid of size 1024×1024. The snapshots are shown at times (a) 0, (b) 0.5, (c) 1, (d) 2, (e) 3, (f) 4, (g) 6, (h) 8 periods, right after the reaction events.

Similar results have been obtained for the acid-base reaction in the same flow, that is, in the case of the exponential stirring protocol. Figure 5 shows a series of snapshots. Initially, the boundary between reactants A and B, populated by product C, is a straight line, which is subsequently stretched and folded into a long, winding filament. Due to stretching, the width of the filaments covered by C decreases, hence A and B can get closer to each other, leading to more reactions $A+B\rightarrow2C$. Eventually, the whole domain becomes covered by C, and the reaction stops.

We can again check the validity of Eq. (27). In Fig. 6 the average concentration c of the product C is shown as a function of time. The chemical decay rate from the figure is σ

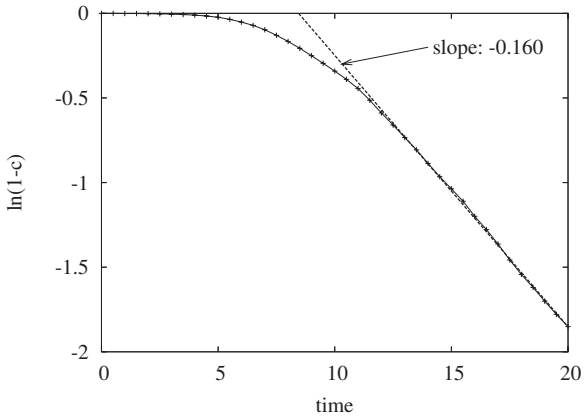

FIG. 6. Concentration c of product C in the acid-base reaction of Fig. 5. Time is measured in periods of the flow, concentration is sampled just after the reaction events. Simulations were performed on a grid of size 8192×8192. The Lyapunov exponent of the flow is $\lambda=0.60\pm0.03$. Crosses represent results obtained from the simulation, the straight line is predicted by Eq. (27). The relaxation exponent from the plot is $\sigma=0.160\pm0.001$.

$=0.160\pm0.001$, which is smaller than the Lyapunov exponent $\lambda=0.60\pm0.02$.

As an example of the linear stirring protocol, Fig. 7 shows a series of snapshots of the autocatalytic process in the velocity field (37) of the vortex pair. The distribution of C particles is stretched by the flow, it forms filaments, but the filaments grow much slower than in the case of the exponential protocol, see Fig. 2. In the comoving frame, the majority of particles remains around the vortices and the flow is thus practically closed.

The average concentration of the autocatalytic particles is, again, well predicted by our theory (27). This is illustrated by Fig. 8, where the chemical decay rate is found to be $\sigma=0.0327\pm0.00004$. This value can be compared to that predicted by Eq. (32). The linear stretching rate is not homogeneous in the velocity field of the vortex pair, but its average is $\lambda\approx2$ for the initial conditions used in the numerical experiments. From this, the dimensionless front velocity in the simulation is $U=v/\lambda L\approx10/2\times8192$, since the front moves forward by ten grid cells of size $1/8192$ in a time interval of length 1. We can estimate that finally a fraction of $\mathcal{H}\approx1/4$ of the observation area is covered by material in the final state (before the filamentary structures are destroyed by the reaction). These give, via Eq. (32), $\sigma\approx\min\{0.14a,0.14\}$, which is in accordance with the measured $\sigma=0.03272\pm0.00004$ for $a\approx0.23$.

V. OPEN FLOWS

The basic new feature in open flows is the escape of particles from any preselected region due to the transport produced by the flow. A persistent product distribution can only be maintained if the passive advection dynamics possesses an invariant set in the region of observation. This must have an unstable manifold along which the particles leave, after being trapped for a long time close to the invariant set. The simplest of such invariant sets is a hyperbolic point (by disregarding specific atypical fixed points). The local stretching and contraction around hyperbolic points is exponential (even if of a special type, see below). The study of the linear protocol is thus not meaningful in open flows since this protocol would lead to an empty asymptotic chemical state. In this section we therefore have $p(l)\equiv1$.

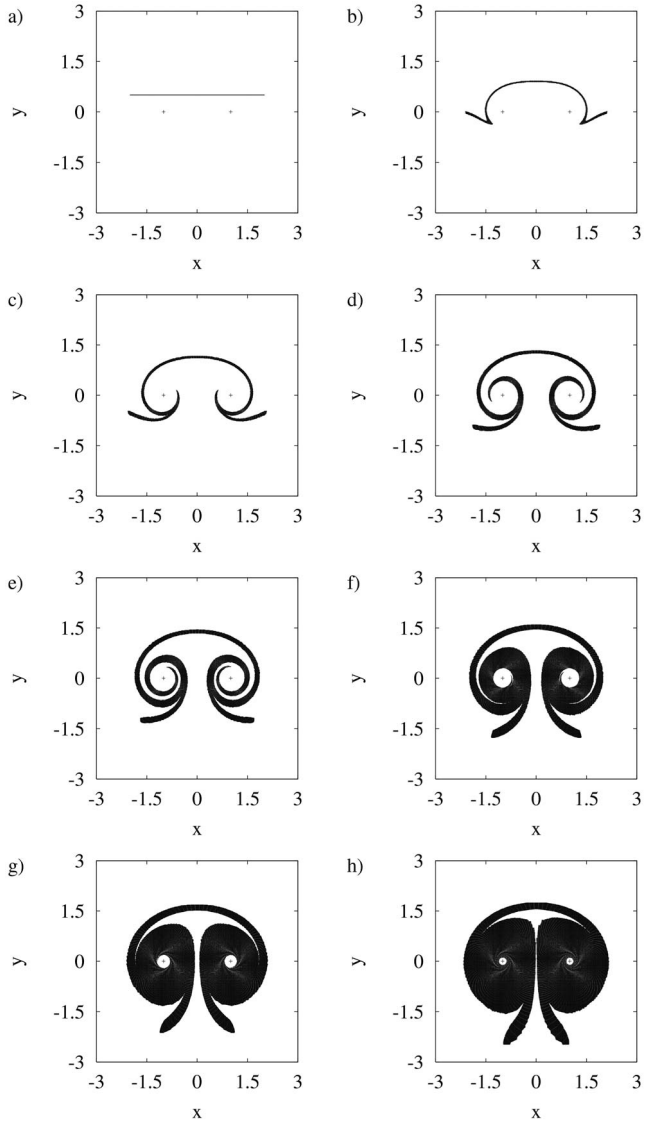

FIG. 7. Distribution of the autocatalytic C particles (black) in a frame comoving with the vortex pair (37). Simulations were performed on a grid of size 1024×1024. Autocatalytic reactions occurred after time intervals of length 0.1. The snapshots are shown at times (a) 0, (b) 0.5, (c) 1, (d) 1.5, (e) 2, (f) 3, (g) 4, (h) 5 right before the reaction events. The locations of the vortex centers are denoted by small crosses.

A measure of the escape process is the so-called escape rate κ governing the exponential decay of the number of particles staying in the neighborhood of an asymptotic set. In chaotic flows, this asymptotic set is a chaotic saddle. The unstable manifold of the saddle is a well defined fractal of some dimension $1<D^{*}<2$ traced out by the particles after long enough time. These quantities and the average Lyapunov exponent λ fulfill the relation [39,41]

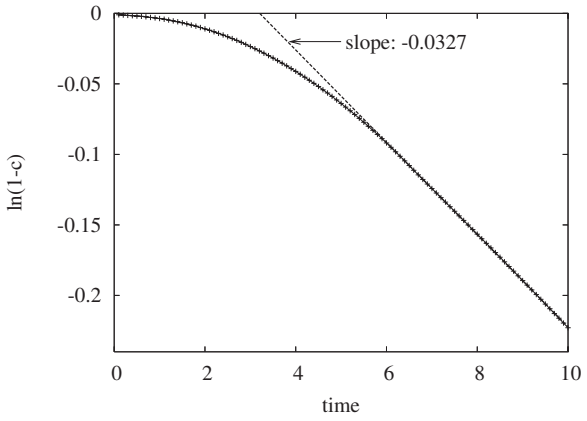

FIG. 8. Concentration c of reactant C in the autocatalytic reaction of Fig. 7. The simulations were performed on a grid of size 8192×8192. Crosses represent results obtained from the simulation, the straight line is predicted by Eq. (27). The relaxation exponent from the plot is $\sigma=0.03272\pm0.00004$.

$$D^* = 2 - \frac{\kappa}{\lambda}. \tag{38}$$

The case of nonchaotic flows with isolated hyperbolic points follows as the special limit of $\kappa\to\lambda$. In view of Eq. (38) this implies $D^*=1$, corresponding to the fact that the unstable manifold of such fixed point is a smooth curve.

The region of observation is a fixed segment of the flow of area $\mathcal{H}L^2$. In the presence of reactions, the dynamics of the local width is unchanged, Eq. (6) remains thus valid. After long enough time, d assumes a fixed value d^*. In analogy with the closed case, the full available asymptotic dimensionless area is $\mathcal{H}^* d^{*2-D^*}$, where $\mathcal{H}^*$ is the Hausdorff volume of the asymptotic set, a dimensionless number. The asymptotic dimensionless concentration c^* is therefore $\bar{c}L^2\mathcal{H}^* d^{*2-D^*}/(\bar{c}\mathcal{H}L^2)$, i.e.,

$$c^* = \frac{\mathcal{H}^*}{\mathcal{H}} d^{*2-D^*}, \tag{39}$$

less than unity. The full dimensionless asymptotic length is accordingly $l^*=\mathcal{H}^* d^{*1-D^*}$.

The effective dimension is defined now from the number of boxes needed to cover the product content with box size $d(t)$ via $N(d)=\mathcal{H}^* d^{-D_{\rm eff}(t)}$. In analogy with Eq. (14) we have for the total time-dependent length

$$l(t) = \mathcal{H}^* d(t)^{1-D_{\rm eff}(t)}. \tag{40}$$

The product content at time t is $C(t)=\bar{c}L^2\mathcal{H}^* d(t)^{2-D_{\rm eff}(t)}$, from which the average dimensionless concentration $c(t)=C(t)/(\bar{c}\mathcal{H}L^2)$ is

$$c(t) = \frac{d(t)l(t)}{\mathcal{H}} = \frac{\mathcal{H}^*}{\mathcal{H}} d(t)^{2-D_{\rm eff}(t)}, \tag{41}$$

as a generalization of Eq. (15). Furthermore, from Eqs. (39)–(41) we find

$$\frac{l(t)}{l^*} = \frac{c(t)d^*}{c^* d(t)}. \tag{42}$$

Thus, the concentration determines both the width and the length as

$$d(t) = \left(c(t)\frac{\mathcal{H}}{\mathcal{H}^*}\right)^{1+\beta(t)} \quad \text{and} \quad l(t) = \mathcal{H}^*\left(c(t)\frac{\mathcal{H}}{\mathcal{H}^*}\right)^{-\beta(t)}, \tag{43}$$

where exponent $\beta(t)$ remains defined via Eq. (17).

The equation for the dimensionless length l differs from Eq. (13) since the stretching rate restricted to the fixed region of observation is not λ. In open chaotic flows the stretching rate is the Lyapunov exponent minus the escape rate, that is, $\lambda-\kappa$ [41]. In open nonchaotic flows $\lambda-\kappa=0$ implying that a material line is quickly stretched across the domain of observation and its length within this domain does not grow any longer (while its width is subjected to an exponential compression up to arbitrarily long times).

Thus we have

$$\dot{l} = (\lambda-\kappa) l f\left(\frac{l}{l^*}\right). \tag{44}$$

The folding function f describes in this case how the area $\mathcal{H}^* d^{*2-D^*}$ around the unstable manifold is filled up by the filaments containing material C.

From the time derivatives of the two sides of Eq. (41), and from Eqs. (6) and (44), we obtain

$$\dot{c} = -c\lambda r(d,l) + (\lambda-\kappa)cf(l/l^*) \tag{45}$$

and

$$\dot{D}_{\rm eff}\ln d = \lambda\left[(D_{\rm eff}-1)r(d,l) - \left(1-\frac{\kappa}{\lambda}\right)f(l/l^*)\right]. \tag{46}$$

If the concentration and the dimension are kept as the basic variables, l and d are to be expressed via Eq. (43).

In order to see how the trivial $c\to c^*$, $D_{\rm eff}\to D^*$, $d\to d^*$ final state is reached, we linearize Eqs. (6) and (45) as

$$\dot{d} = -\lambda\left(y d^* - z\frac{c^*\mathcal{H}}{d^*}\right)(d-d^*) - \lambda z\mathcal{H}(c-c^*), \tag{47}$$

$$\dot{c} = -\left(\lambda c^* y - \lambda z\frac{c^{*2}\mathcal{H}}{d^{*2}} - (\lambda-\kappa)\frac{ac^*}{d^*}\right)(d-d^*) - \left(\lambda z\frac{c^*\mathcal{H}}{d^*} + (\lambda-\kappa)a\right)(c-c^*), \tag{48}$$

and the shorthand notations are the ones introduced after Eq. (25). The dimension is found, again, to follow the width and concentration dynamics since

$$\dot{D}_{\rm eff} = -\frac{1}{\ln d^*}\left(\frac{\dot{c}}{c^*} - (2-D^*)\frac{\dot{d}}{d^*}\right). \tag{49}$$

The eigenvalues are obtained as $-y\lambda d^*$ and $-(\lambda-\kappa)a$. The chemical decay rate is thus

$$\sigma = \lambda \min\left\{a\left(1 - \frac{\kappa}{\lambda}\right), yd^*\right\}. \tag{50}$$

In view of Eq. (38), this can be written as

$$\sigma = \lambda \min\{a(D^* - 1), 1\}, \tag{51}$$

$$\sigma = \lambda \min\{a(D^* - 1), 2\}, \tag{52}$$

for the autocatalytic and the acid-base reactions, respectively, which shows that the value of the asymptotic fractal dimension is also important in the determination of the decay rate.

In the special case of nonchaotic flows with hyperbolic points [see Eq. (44)] the eigenvalue proportional to a does not appear, and we have

$$\sigma = \lambda \quad \text{and} \quad \sigma = 2\lambda \tag{53}$$

for the autocatalytic and the acid-base reactions, respectively. The asymptotic convergence is exponential in this nonchaotic case as well, although $D_{\text{eff}}(t) \equiv 1$ at any time.

We note that Eqs. (45) and (46) also contain the equation obtained previously [7,35] for reactions in open chaotic flows. In that case, the effective dimension was assumed to be the time-independent information dimension D^* of the unstable manifold, from the very beginning of the monitoring of the reaction dynamics. From $D_{\text{eff}} \equiv D^*$ [cf. Eq. (38)] and $\dot{D}_{\text{eff}} \equiv 0$ in Eq. (46), we obtain $f=r$. With this constraint Eq. (45) yields

$$\dot{c} = -\kappa c r(d,l). \tag{54}$$

In the frontal (autocatalytic) reaction case $r=1-2U/d$, and hence we find

$$\dot{c} = -\kappa c + 2U\kappa q c^{-\beta^*} \tag{55}$$

with $q=(\mathcal{H}^*/\mathcal{H})^{(1+\beta^*)}$ as a geometrical parameter. For acid-base reactions

$$\dot{c} = -\kappa c + \frac{\kappa}{\text{Pe}} q c^{-1-2\beta^*}, \tag{56}$$

where $q=(\mathcal{H}^*/\mathcal{H})^{2(1+\beta^*)}$. These expressions, and in particular Eq. (55), have been numerically investigated and found to well approximate the asymptotic behavior [23].

It is interesting to investigate the approach of the steady state in this restricted dynamics. By linearizing Eq. (54) and using the fact that in view of Eq. (49) $(c-c^*)/c^*=(2-D^*)(d-d^*)/d^*$, we obtain the chemical decay rate as $\sigma' = y\lambda d^*$. We see that the restricted dynamics preserves one of the eigenvalues. It is the saturation process which is not taken into account, and consequently it is the eigenvalue proportional to parameter a which does not appear.

VI. SUMMARY

One of the features of this study is the extension of the theory to nonchaotic flows with linear stirring protocol. A remarkable observation is that the product becomes distributed on fractal filaments before reaching the asymptotic steady state in spite of the fact that there is no fractal (chaotic) invariant set present in such flows. We carried out simulations (not shown) in chaotic flows which contained large KAM islands (linear protocol) within the chaotic band (exponential protocol). In flows with such divided phase space the chemical decay was found to follow the rule characteristic of the exponential protocol, implying that the contribution from the linear protocol was suppressed.

The equations of motion (18) and (20) imply a scaling form. A rescaling of time indicates that the basic variable is λt, and as parameters d^* and $\mathcal{H}$ can appear. Consequently,

$$c(t,\lambda,d^*,\mathcal{H}) = g(\lambda t, d^*, \mathcal{H}), \tag{57}$$

and similarly for $\beta(t)$. In the exponential protocol, a further simplification occurs because the protocol and reaction functions are independent of the length l. Therefore, $\mathcal{H}$ does not show up and

$$c(t,\lambda,d^*) = g(\lambda t, d^*). \tag{58}$$

As our asymptotic analysis has shown, the d^* dependence disappears for long times (and $d^*/\mathcal{H}$ remains the only parameter of the linear protocol case).

The predicted exponential-type asymptotic behavior of the chemical product has been found for acid-base reactions in closed flows in the numerical simulations of Ref. [10]. Also, a similar asymptotic behavior and initial linear growth of the chemical product in closed containers have been observed in the experiments by Arratia and Gollub [4] also for acid-base reactions. They apply a fit of the form $1-c \sim \exp(-At-Bt^2)$ from an early stage up to the very end, and find a nonzero coefficient B. This is not directly comparable with the asymptotic statements of our theory. A fit to our numerical results from an early stage is also possible with their formula but the sign of coefficient A is negative. In any case, coefficient A is basically different from the chemical decay rate σ governing the asymptotic behavior.

Similar results are expected in the experimental investigation of autocatalytic reactions as well. We hope also that the fractal kinetics of reactions in nonchaotic flows can also be investigated experimentally in the near future. A good candidate of the latter could be the experiment by Rogers and Morris [32].

ACKNOWLEDGMENTS

Useful discussions with J. Gollub, P. Arratia, A. P. S. de Moura, I. Benczik, I. Scheuring, Z. Neufeld, T. Solomon, C. Grebogi, and E. Villermaux are acknowledged. This research has been supported by OTKA Grants Nos. T047233, TS044839, F042476, and T046646. Gy.K. was supported by a Bolyai grant and by the Medical Research Council in the UK.

[1] O. Paireau and P. Tabeling, Phys. Rev. E **56**, 2287 (1997).
[2] C. R. Nugent, W. M. Quarles, and T. H. Solomon, Phys. Rev. Lett. **93**, 218301 (2004).
[3] M. S. Paoletti and T. H. Solomon, Europhys. Lett. **69**, 819 (2005); M. S. Paoletti and T. H. Solomon, Phys. Rev. E **72**, 046204 (2005).
[4] P. E. Arratia and J. P. Gollub, Phys. Rev. Lett. **96**, 024501 (2006); C. Day, Phys. Today **59**, 15 (2006).
[5] M. S. Paoletti, C. R. Nugent, and T. H. Solomon, Phys. Rev. Lett. **96**, 124101 (2006).
[6] G. Metcalfe and J. M. Ottino, Phys. Rev. Lett. **72**, 2875 (1994); F. J. Muzzio and M. Liu, Chem. Eng. J. **64**, 117 (1996).
[7] Z. Toroczkai, G. Karolyi, A. Pentek, T. Tel, and C. Grebogi, Phys. Rev. Lett. **80**, 500 (1998).
[8] Z. Neufeld, Phys. Rev. Lett. **87**, 108301 (2001).
[9] A. Wonhas and J. C. Vassilicos, Phys. Rev. E **65**, 051111 (2002).
[10] M. Giona, S. Cerbelli, and A. Adrover, J. Phys. Chem. A **106**, 5722 (2002).
[11] I. Z. Kiss, J. H. Merkin, and Z. Neufeld, Phys. Rev. E **70**, 026216 (2004).
[12] C. R. Koudella and Z. Neufeld, Phys. Rev. E **70**, 026307 (2004).
[13] I. J. Benczik, Z. Neufeld, and T. Tél, Phys. Rev. E **71**, 016208 (2005).
[14] A. V. Straube, M. Abel, and A. Pikovsky, Phys. Rev. Lett. **93**, 174501 (2004).A. V. Straube and A. Pikovsky, e-print arXiv:0706.4274v1
[15] Gy. Károlyi and T. Tél, Phys. Rev. Lett. **95**, 264501 (2005).
[16] I. J. Benczik, Phys. Rev. E **71**, 066205 (2005).
[17] A. Vikhansky and S. M. Cox, Phys. Fluids **18**, 037102 (2006).
[18] S. M. Cox, Phys. Rev. E **74**, 056206 (2006).
[19] M. Sandulescu, E. Hernández-García, C. López, and U. Feudel, Tellus, Ser. A **58**, 605 (2006); M. Sandulescu, C. López, E. Hernández-García, and U. Feudel (unpublished).
[20] S. N. Menon and G. A. Gottwald, Phys. Rev. E **75**, 016209 (2007).
[21] V. Perez-Munuzuri and G. Fernandez-Garcia, Phys. Rev. E **75**, 046209 (2007).
[22] M. Vergassola, E. Villermaux, and B. I. Shraiman, Nature (London) **445**, 406 (2007).
[23] T. Tél, A. M. de Moura, C. Grebogi, and G. Károlyi, Phys. Rep. **413**, 91 (2005).
[24] E. Villermaux and Y. Gagne, Phys. Rev. Lett. **73**, 252 (1994); E. Villermaux and C. Innocenti, J. Fluid Mech. **393**, 123 (1999).
[25] A. E. Motter, Y.-C. Lai, and C. Grebogi, Phys. Rev. E **68**, 056307 (2003).
[26] A. P. S. de Moura and C. Grebogi, Phys. Rev. E **70**, 036216 (2004).
[27] A. E. Motter, A. P. S. de Moura, C. Grebogi, and H. Kantz, Phys. Rev. E **71**, 036215 (2005).
[28] G. Károlyi, Phys. Rev. E **71**, 031915 (2005).
[29] P. Meinier and E. Villermaux, J. Fluid Mech. **476**, 213 (2003).
[30] E. Villermaux and H. Rehab, J. Fluid Mech. **425**, 161 (2000).
[31] E. Villermaux and J. Duplat, Phys. Rev. Lett. **91**, 184501 (2003).
[32] M. C. Rogers and S. W. Morris, Phys. Rev. Lett. **95**, 024505 (2005).
[33] J. P. Crimaldi, J. R. Hartford, and J. B. Weiss, Phys. Rev. E **74**, 016307 (2006).
[34] D. Martinand and J. C. Vassilicos, Phys. Rev. E **75**, 036315 (2007).
[35] T. Tél *et al.*, Chaos **10**, 89 (2000); **14**, 72 (2004).
[36] M. C. Cross and P. C. Hohenberg, Rev. Mod. Phys. **65**, 851 (1993).
[37] R. M. Anderson and R. M. May, *Infectious Diseases of Humans* (Oxford University Press, Oxford, 1992).
[38] M. Liu, F. J. Muzzio, and R. L. Peskin, Chaos, Solitons Fractals **4**, 869 (1994); R. Pierrehumbert, *ibid.* **4**, 1091 (1994).
[39] E. Ott, *Chaos in Dynamical Systems* (Cambridge University Press, Cambridge, 1993).
[40] P. Newton, *The N-Vortex Problem* (Springer, Berlin, 2001).
[41] T. Tél and M. Gruiz, *Chaotic Dynamics* (Cambridge University Press, Cambridge, 2006).